Eur. Phys. J. A **31**, 195–202 (2007)
DOI 10.1140/epja/i2006-10171-0

THE EUROPEAN PHYSICAL JOURNAL A

Regular Article – Nuclear Structure and Reactions

Single-particle spin effect on fission fragment angular momentum

H. Naik[a], S.P. Dange, R.J. Singh, and A.V.R. Reddy

Radiochemistry Division, Bhabha Atomic Research Centre, Trombay, Mumbai-400085, India

Received: 5 July 2006 / Revised: 20 November 2006
Published online: 9 February 2007 – © Società Italiana di Fisica / Springer-Verlag 2007
Communicated by C. Signorini

Abstract. Independent isomeric yield ratios (IYR) of ^{128}Sb, ^{130}Sb, ^{132}Sb, ^{131}Te, ^{133}Te, ^{132}I, ^{134}I, ^{136}I, ^{135}Xe, and ^{138}Cs have been determined in the fast neutron-induced fission of ^{243}Am using the radiochemical and γ-ray spectrometric technique. From the IYR, fragment angular momenta ($J_{\rm rms}$) have been deduced using the spin-dependent statistical model analysis. From the $J_{\rm rms}$-values and experimental kinetic energy data deformation parameters (β) have been deduced using the pre-scission bending mode oscillation model and the statistical model. The $J_{\rm rms}$- and β-values of fission fragments from the present and earlier work in the odd-Z fissioning systems (^{238}Np*, ^{242}Am* and ^{244}Am*) are compared with the literature data in the even-Z fissioning systems (^{230,233}Th*, ^{233,234,236,239}U*, ^{239,240,241,242}Pu*, ^{244}Cm(SF), ^{245,246}Cm*, ^{250}Cf* and ^{252}Cf(SF)) to examine the role of single-particle (proton) spin effect. It was observed that i) in all the fissioning systems $J_{\rm rms}$- and β-values of the fragments with spherical 82n shell and even-Z products are lower than the fragments away from the spherical neutron shell and odd-Z products, which indicate the effect of nuclear structure. ii) For both even-Z and odd-Z fission products $J_{\rm rms}$-values increase with ${Z_{\rm F}}^2/A_{\rm F}$ due to increase in Coulomb torque. iii) The $J_{\rm rms}$- and β-values of even-Z fission products are comparable in all the fissioning systems. However, for odd-Z fission products they are slightly higher in the odd-Z fissioning systems compared to their adjacent even-Z fissioning systems. This is possible due to the contribution of the extra single-particle (proton) spin of the odd-Z fissioning systems to their odd-Z fragments. iv) The yield-weighted fragment angular momentum and elemental yields profile shows an anti-correlation in even-Z fissioning systems but not in the odd-Z fissioning systems.

PACS. 25.85.Ec Neutron-induced fission

Introduction

The fragment angular momentum in low-energy fission arises due to the statistical population of various collective modes such as wriggling, bending and twisting [1] besides some contribution from post-scission Coulomb torque [2, 3] and/or single-particle excitation. Thus, studies on the fragment angular momentum in low-energy fission of actinides provide information about the effect of rotational degrees besides single-particle effect. Experimental investigations on the fission fragment angular momentum have been carried out using different physical [3–14] and radiochemical [15–30] methods. The physical method based on the measurements of anisotropy [3,4] and multiplicity [5–7] of the prompt γ-rays provides the angular momentum of the mass-averaged fission products. The fragment angular momentum of only even-even fission products has been estimated from the physical method based on the population of rotational band transition intensities [8–10] measured using the multi-parameter coincidence technique and employing the statistical model analysis. On the other hand, the fragment angular momentum of both even-Z and odd-Z fission products with specific mass and charge has been obtained [11–30] from their independent isomeric yields ratio by employing the statistical model analysis. The determination of the fragment angular momentum from the measured independent isomeric yield ratios for short-lived fission products is based on the physical techniques such as recoil mass separator [11–13] and isotope separator [14]. On the other hand, for long-lived fission products the determination of the fragment angular momentum from the measured independent isomeric yield ratios is based on the radiochemical method and the off-line γ-ray spectrometric technique [15–30]. Using the above methods, the fragment angular momentum of various fission products has been determined in a wide range of even-Z fissioning systems from ^{230}Th* to ^{250}Cf* [25–29] and in two odd-Z fissioning systems ^{238}Np* and ^{242}Am* [30]. From these data it is clear that the fragment angular momentum in low-energy fission shows a correlation with nuclear-structure effects such as the odd-even effect [20–30], shell closure proximity [19–30], quadrupole moment [8], scission point deformation [25–30] and fragment kinetic (ex-

[a] e-mail: naikh@barc.gov.in

citation) energy [11–13]. Besides these, an anti-correlation between the fragment angular momentum and elemental yields was observed in fifteen even-Z fissioning systems [25–29] due to the coupling between the collective and the intrinsic degree of freedom. It is worth to examine such aspects in the odd-Z fissioning systems, where the proton even-odd effect on the elemental yields profile is not expected [31,32]. During our earlier work [30] on the fragment angular momentum in ^{238}Np* and ^{242}Am*, elemental yields were not available for these fissioning systems to examine the above aspects. During that time elemental yields of light-mass elements were available in ^{239}Np* [31], where the fission fragment angular momenta of the fission products were not determined. Recently, elemental yields of heavy-mass fission product elements have been determined in the odd-Z fissioning systems such as ^{238}Np*, ^{242}Am* and ^{244}Am* [32]. Among these fissioning systems, the data on the fragment angular momentum is not available in ^{244}Am*. In view of the above fact, in the present work, the fragment angular momenta of ^{128}Sb, ^{130}Sb, ^{132}Sb, ^{131}Te, ^{133}Te, ^{134}I, ^{136}I, ^{135}Xe and ^{138}Cs in the fast neutron-induced fission of ^{243}Am have been deduced from the independent isomeric yield ratios determined using the radiochemical and off-line γ-ray spectrometric technique. These data and similar data from earlier work [30] in odd-Z fissioning systems are compared with the data of even-Z fissioning systems [28,29] to examine the role of single-particle spin. The correlation between the fragment angular momentum and elemental yields has also been discussed in both even-Z and odd-Z fissioning systems.

Experiment and calculations

For short-lived fission products the nitrate solution of ^{243}Am ($\sim 50\,\mu$g) was sealed in a polypropylene tube and wrapped with 1 mm thick cadmium foil. They were additionally sealed in alkathene bags and irradiated for 3 to 5 minutes with a neutron flux of $5 \times 10^{12}\,\mathrm{cm^{-2}\,s^{-1}}$ using the pneumatic carrier facility of the reactor CIRUS. The cadmium wrapper was used to cut off thermal neutrons and avoid the contribution from the thermal neutron-induced fission of ^{243}Am. The irradiated solution in the sealed polypropylene tube was then mounted on a Perspex plate or used for the radiochemical separation of cesium [20, 30]. The separated cesium sample and the sealed irradiated solution on the Perspex plate were counted at a fixed geometry on an energy- and efficiency-calibrated 80 c.c. HPGe detector coupled to a PC-based 4096-channel analyzer in live time mode. The resolution of the detector system was 2.0 keV at 1332 keV of ^{60}Co. For long-lived fission products electrodeposited targets of ^{243}Am ($\sim 90\,\mu$g) were covered with $25\,\mu$m thick aluminum foil or $75\,\mu$m thick Lexan foil, which act as a catcher to collect the recoiling fission products during the neutron irradiation of the targets. They were then wrapped with 1 mm thick cadmium foil, doubly sealed in alkathene bags and irradiated for 5 to 60 minutes in the reactor APSARA at a neutron flux of $1.2 \times 10^{12}\,\mathrm{cm^{-2}\,s^{-1}}$. After the irradiation, the aluminum catcher foil was used for the radiochemical separation of tellurium and iodine [23–25,33]. On the other hand, the Lexan catcher foil was washed with very dilute nitric acid and distilled water to remove any possible contamination of ^{243}Am and was then mounted on a Perspex plate. Standard aliquots of separated tellurium and iodine solution in counting vials as well as the mounted Lexan catcher on the Perspex plate were counted at a fixed geometry on an energy- and efficiency-calibrated 120 c.c. HPGe detector coupled to a PC-based 4096-channel analyzer in live time mode. The resolution of the detector system was 1.8 keV at 1332 keV of ^{60}Co. The dead time was always kept at less than 10% to avoid a pile-up effect. In the γ-ray spectrum of the irradiated solution the γ-ray background of ^{239}Np from ^{243}Am makes it difficult to analyze the fission products having a γ-ray energy below 350 keV [34]. The γ-ray spectrum of the irradiated solution in the sealed polypropylene tube was taken to measure the short-lived fission products and the inert gas fission products, which otherwise escape in other types of irradiation. On the other hand, in the γ-ray spectrum of the Lexan catcher foil, the presence of γ-lines of ^{239}Np was not seen [34] and therefore it could be used to measure fission products of relatively longer-lived fission products. The γ-lines along with the nuclear spectroscopic data for the different fission products used in the present work are taken from refs. [35,36].

The photo-peak areas of the γ-rays for the radionuclides of present interest were calculated from their total peak areas by subtracting the Compton background. From the photo-peak areas, independent isomeric yields and thus their ratios were calculated using the standard decay growth equation [15–30] after correcting for the precursor contribution. The activities of ^{92}Sr and ^{104}Tc were used as the fission rate monitors in the long- and short-irradiated un-separated samples, respectively. On the other hand, in the separated samples of tellurium, iodine and cesium samples ^{134}Te, ^{135}I and ^{139}Cs were used as fission rate monitors, respectively. The cumulative yields of the precursor were either determined in the present work or taken from the literature [34,37–39].

Results and discussion

The independent isomeric yield ratios (IYR) of ^{128}Sb, ^{130}Sb, ^{132}Sb, ^{131}Te, ^{133}Te, ^{132}I, ^{134}I, ^{136}I, ^{135}Xe and ^{138}Cs in the fast neutron-induced fission of ^{243}Am determined in the present work using the radiochemical and off-line γ-ray spectrometric technique are given in table 1. The uncertainty on the IYR includes the error due to counting statistics, absolute abundance of the γ-lines, detector efficiencies, the fission yields of the precursor and the least square fit analysis. From the independent isomeric yield ratios, fragment angular momenta (J_{rms}) were deduced using the spin-dependent statistical model analysis [40] and are given in table 1. The IYR and J_{rms} of the above-mentioned fission products in the other two odd-Z fissioning systems (^{238}Np* and ^{242}Am*) from our earlier work [30] are also given in table 1 for comparison. The

Table 1. Independent isomeric yield ratio (IYR), fragment angular momentum ($J_{\rm rms}$) and different parameters related to the scission point configuration in ^{238}Np*, ^{242}Am* and ^{244}Am*.

Nuclide	IY(%)	IYR	Ref.[b]	$J_{\rm rms}$	β	c	T	K.E. (MeV)	
	$(Y_{\rm h}+Y_{\rm l})$[a]	$Y_{\rm h}/(Y_{\rm h}+Y_{\rm l})$		($\hbar$)		(F)	(MeV)	Calc.	Exp.
^{238}Np*									
^{128}Sb	0.410 ± 0.086	0.518 ± 0.080	[30]	10.2 ± 1.3	0.73	1.05	0.75	176.9	176.0
^{130}Sb	1.414 ± 0.250	0.470 ± 0.157	[30]	9.5 ± 1.9	0.59	1.06	0.73	178.6	178.0
^{132}Sb	1.732 ± 0.186	0.377 ± 0.085	[30]	7.5 ± 1.0	0.17	1.07	0.68	180.3	181.0
^{131}Te	1.576 ± 0.214	0.653 ± 0.056	[30]	5.5 ± 0.4	0.13	1.06	0.69	178.2	178.0
^{133}Te	3.743 ± 0.135	0.570 ± 0.027	[30]	4.7 ± 0.3	0.001	1.12	0.62	188.3	180.0
^{132}I	0.540 ± 0.024	0.486 ± 0.047	[30]	8.9 ± 0.7	0.70	1.08	0.71	181.1	181.0
^{134}I	2.817 ± 0.248	0.429 ± 0.071	[30]	8.2 ± 1.1	0.31	1.07	0.68	179.4	179.5
^{136}I	3.561 ± 0.338	0.684 ± 0.105	[30]	8.4 ± 1.5	0.33	1.06	0.68	177.7	178.5
^{135}Xe	0.401 ± 0.073	0.613 ± 0.130	[30]	5.0 ± 1.5	0.011	1.07	0.64	180.5	179.0
^{138}Cs	1.738 ± 0.038	0.703 ± 0.084	[30]	9.8 ± 1.5	0.62	1.06	0.70	176.4	176.0
^{242}Am*									
^{128}Sb	0.375 ± 0.029	0.575 ± 0.166	[30]	11.1 ± 2.4	0.93	1.07	0.75	184.9	185.0
^{130}Sb	1.194 ± 0.182	0.506 ± 0.137	[30]	10.0 ± 2.0	0.73	1.08	0.72	186.6	186.0
^{132}Sb	1.519 ± 0.120	0.385 ± 0.072	[30]	7.6 ± 0.9	0.19	1.08	0.67	186.6	187.0
^{131}Te	1.446 ± 0.108	0.694 ± 0.078	[30]	5.9 ± 0.7	0.27	1.08	0.68	186.3	186.5
^{133}Te	3.378 ± 0.316	0.583 ± 0.037	[30]	4.9 ± 0.5	0.011	1.08	0.65	186.3	186.5
^{132}I	0.323 ± 0.043	0.526 ± 0.038	[30]	9.5 ± 0.5	0.64	1.09	0.70	187.6	187.0
^{134}I	2.458 ± 0.228	0.465 ± 0.047	[30]	8.7 ± 0.5	0.44	1.08	0.68	185.9	185.7
^{136}I	3.618 ± 0.187	0.743 ± 0.113	[30]	9.7 ± 2.1	0.63	1.07	0.70	184.2	184.0
^{135}Xe	1.728 ± 0.217	0.622 ± 0.138	[30]	5.4 ± 1.6	0.12	1.08	0.66	185.4	185.0
^{138}Cs	2.653 ± 0.087	0.719 ± 0.088	[30]	10.2 ± 1.9	0.71	1.06	0.70	181.4	182.0
^{244}Am*									
^{128}Sb	0.205 ± 0.014	0.594 ± 0.067	A	11.6 ± 1.3	0.98	1.05	0.77	180.8	181.3
^{130}Sb	1.025 ± 0.171	0.515 ± 0.091	A	10.2 ± 1.6	0.75	1.07	0.73	184.3	183.5
^{132}Sb	2.122 ± 0.095	0.383 ± 0.025	A	7.6 ± 0.4	0.17	1.07	0.68	184.3	184.0
^{131}Te	1.255 ± 0.283	0.662 ± 0.099	A	5.6 ± 1.2	0.17	1.07	0.68	183.9	183.7
^{133}Te	3.150 ± 0.481	0.576 ± 0.080	A	4.8 ± 0.7	0.001	1.10	0.64	189.1	184.3
^{132}I	0.201 ± 0.012	0.536 ± 0.041	A	9.7 ± 0.6	0.65	1.07	0.71	183.5	184.0
^{134}I	1.571 ± 0.171	0.458 ± 0.059	A	8.7 ± 0.9	0.43	1.07	0.69	183.5	184.0
^{136}I	4.534 ± 0.636	0.767 ± 0.104	A	10.3 ± 1.8	0.74	1.07	0.70	183.5	183.0
^{135}Xe	0.477 ± 0.076	0.632 ± 0.056	A	5.2 ± 0.7	0.06	1.07	0.66	183.0	183.5
^{138}Cs	2.314 ± 0.278	0.738 ± 0.091	A	10.8 ± 1.9	0.81	1.06	0.71	180.7	180.5

[a] $Y_{\rm h}$ and $Y_{\rm l}$: yield of high- and low-spin isomer, respectively; IY: independent yield.

[b] A: present work; other symbols see text.

$J_{\rm rms}$ of the above fission products in the fissioning systems ^{244}Am* from the present work are determined for the first time.

It can be seen from table 1 that in all the three odd-Z fissioning systems (^{238}Np*, ^{242}Am* and ^{244}Am*) the $J_{\rm rms}$ of odd-Z fission products (^{128,130,132}Sb, ^{132,134,136}I and ^{138}Cs) are higher than the even-Z fission products (^{131,133}Te and ^{135}Xe). In order to examine this aspect the yield-weighted angular momentum of different elements in the odd-Z fissioning systems (^{238}Np* and ^{242,244}Am*) from present and earlier work [30] and in the even-Z fissioning systems (^{230,233}Th*, ^{233,234,236,239}U*, ^{239,240,241,242}Pu*, ^{244}Cm(SF), ^{245,246}Cm*, ^{250}Cf* and ^{252}Cf(SF)) from the literature [25–29] are given in table 2. They are plotted in fig. 1 as a function of the atomic number. It can be seen from fig. 1 that in fifteen even-Z fissioning systems and three odd-Z fissioning systems the $J_{\rm rms}$ of the odd-Z elements are higher than those of the even-Z elements. Higher $J_{\rm rms}$ of the odd-Z elements in both even-Z and odd-Z fissioning systems are due to the polarization of the even-Z core by an odd proton as mentioned by Madsen and Brown [41]. If higher $J_{\rm rms}$ of the odd-Z fragments

Table 2. Yield-weighted average fragment angular momenta of heavy-mass elements in fifteen even-Z and three odd-Z fissioning systems. A: present work; the rest is from other references.

Nuclide	In	Sn	Sb	Te	I	Xe	Cs	Ba	Ce	Nd	Pm	Sm	Ref.
^{230}Th*	–	–	7.49	4.76	8.11	4.7	8.7	–	–	–	–	–	[28]
^{233}Th*	–	–	8.02	4.61	8.89	4.7	9.0	–	–	–	–	–	[29]
^{233}U*	–	–	8.67	5.08	7.87	5.05	9.5	–	–	–	–	–	[29]
^{234}U*	–	–	7.74	4.93	8.01	4.86	10.1	–	–	–	11.8	–	[28]
^{236}U*	6.76	5.7	6.77	4.98	8.15	5.5	10.0	–	–	–	11.0	–	[28]
^{239}U*	–	–	7.28	4.73	8.2	5.3	9.2	–	–	–	–	–	[29]
^{238}Np*	–	–	8.61	4.94	8.36	5.0	9.8	–	–	–	–	–	[30]
^{239}Pu*	–	–	8.72	4.83	8.33	5.15	9.1	–	–	–	–	–	[29]
^{240}Pu*	–	–	8.27	5.27	8.45	5.13	9.35	–	–	–	–	–	[28]
^{241}Pu*	–	–	7.86	5.08	7.91	4.95	9.5	–	–	–	–	–	[29]
^{242}Pu*	–	–	6.53	4.38	8.12	5.45	8.9	–	–	–	–	–	[28]
^{242}Am*	–	–	8.95	5.20	9.31	5.40	10.2	–	–	–	–	–	[30]
^{244}Am*	–	–	8.64	5.03	9.88	5.2	10.8	–	–	–	–	–	A
^{244}Cm	–	–	8.49	4.87	8.7	5.8	8.7	–	–	–	–	–	[26]
^{245}Cm*	–	–	8.61	5.06	9.24	5.8	9.7	–	–	–	–	–	[29]
^{246}Cm*	–	–	9.03	4.96	8.53	5.85	8.9	–	–	–	–	–	[28]
^{250}Cf*	–	–	12.35	5.69	8.4	6.4	9.3	–	–	–	9.7	–	[28]
^{252}Cf	–	–	8.06	4.55	9.97	7.83	7.9	7.24	8.87	9.39	–	11.1	[28]

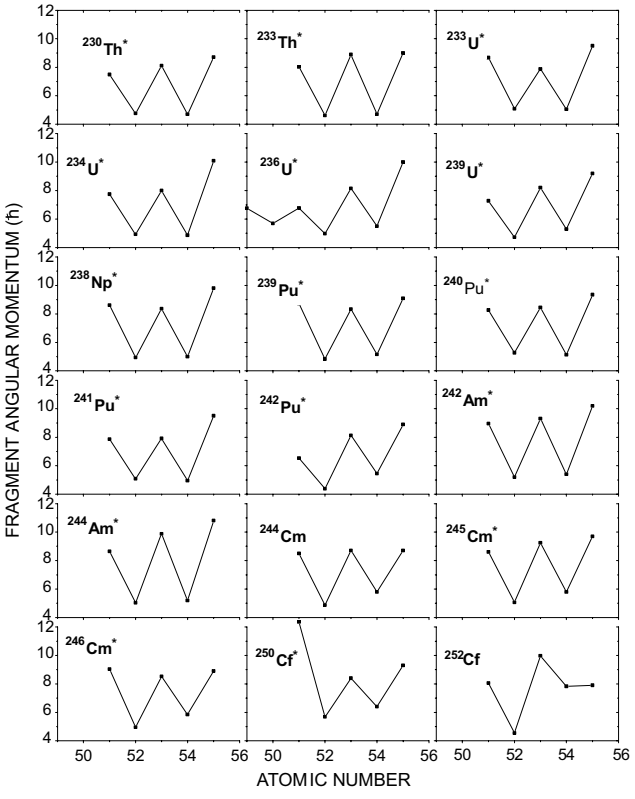

Fig. 1. Plot of yield-weighted average fragment angular momenta as a function of the atomic number in fifteen even-Z fissioning systems and three odd-Z fissioning systems.

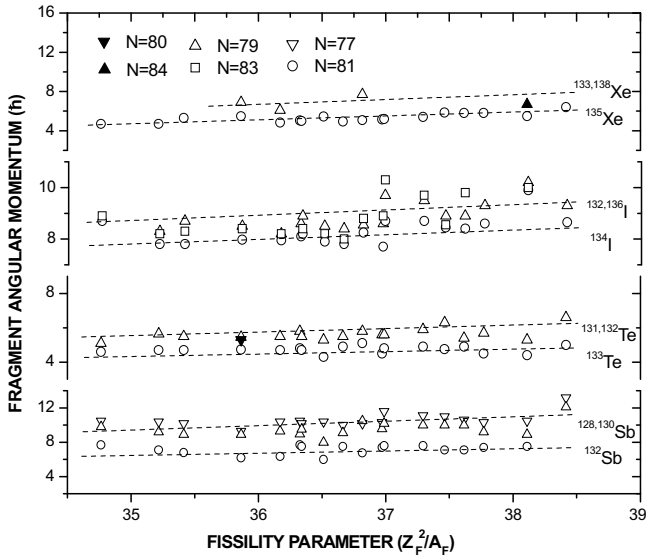

Fig. 2. Plot of the fragment angular momentum of various Sb, Te, I and Xe isotopes as a function of the fissility parameter $({Z_{\rm F}}^2/A_{\rm F})$. (The data in the fissioning systems ^{244}Am* is from the present work).

are due to deformation then spherical fragments should show a lower angular momentum and deformed fragments should show a higher angular momentum. In view of this, the $J_{\rm rms}$ of various isotopes of Sb, Te, I and Xe are plotted in fig. 2 as a function of the fissility parameter $({Z_{\rm F}}^2/A_{\rm F})$. The limits of error are not shown in the fig. 2 to avoid clumsiness. In fig. 2 the fragment angular momenta of various fission products in the fissioning system ^{244}Am* are from the present work. From fig. 2 it can be seen that the fragment angular momentum increases with the increase of the fissility parameter $({Z_{\rm F}}^2/A_{\rm F})$. This may be

due to the increase of the Coulomb torque with the increase of ${Z_{\rm F}}^2/A_{\rm F}$. It can be also seen from fig. 2 that in all the fissioning systems $J_{\rm rms}$ of ^{132}Sb, ^{133}Te, ^{134}I and ^{135}Xe seem to be lower than those of ^{128,130}Sb, ^{131,132}Te, ^{132,136}I and ^{133,138}Xe, respectively. From the bending mode oscillation [2] it is expected that heavy-mass fragments should have a higher angular momentum than lighter-mass fragments. The contradictory observation [18–30] of a lower angular momentum of ^{132}Sb, ^{133}Te, ^{134}I and ^{135}Xe than of ^{128,130}Sb, ^{131}Te, ^{132}I and ^{133}Xe is due to the presence of a spherical 82n shell in the fragment stage of the former products, since the number of neutrons emitted in the mass range of 132–135 are about one. This indicates the effect of shell closure proximity on deformation as expected above. The role of fragment deformation was observed earlier [8,25] from the higher $J_{\rm rms}$ of the fission products ^{111,112}Pd, ^{140}Xe and ^{142}Ba compared to ^{114,116}Pd, ^{135}Xe and ^{144,146}Ba in ^{252}Cf(SF). This is because the fission products ^{111,112}Pd, ^{140}Xe and ^{142}Ba have either deformed 66n or 88n shell in their fragment stage [8,25] if one considers one to two neutron emissions in these mass regions. The role of fragment deformation gets support from the higher $J_{\rm rms}$ of super deformed fragments such as ^{104}Mo and ^{144,146}Ba in ^{252}Cf(SF) [9,10]. Higher $J_{\rm rms}$ of permanently deformed rare-earth fission products such as ^{148}Pm in ^{234,236}U* [16], ^{154}Pm in ^{250}Cf* [28] as well as ^{146,148,150}Ce, ^{152,154}Nd and ^{156}Sm in ^{252}Cf(SF) [8] also support the above fact. The decrease of the fragment angular momentum with the increase of the kinetic energy in ^{234,236}U* and ^{240}Pu* [11–14] further supports this fact. All these observations clearly indicate that the fragment angular momentum is related to the nuclear-structure effect through the single-particle effect and/or fragment deformation at the scission. In view of this, the deformation parameters (β) were calculated from the $J_{\rm rms}$-values and kinetic energy data and using statistical as well as prescission bending mode oscillation models as done in our earlier work [25–30].

Based on the statistical equilibrium among various collective modes [1] the root mean square angular momentum ($J_{\rm rms}$) is given as [8]

$$J_{\rm rms} = 2IT/\hbar^2\,, \tag{1}$$

where I is the temperature- (T) dependent moment of inertia related to the fragment excitation energy (E^*) as [19, 20]

$$I = I_{\rm rig}[1-0.8\exp(-0.693E^*/5)] \quad \text{and} \quad E^* = aT^2, \tag{2}$$

$$I_{\rm rig} = (2/5)Mz^2 \quad \text{and} \quad M = r_0A^{1/3}\,, \tag{3}$$

where $I_{\rm rig}$ is the rigid-body moment of inertia, a is the level density parameter taken as $a = A/8\,{\rm MeV}^{-1}$, r_0 is the radius constant taken as 1.2249 F [42], M is the mass of the fragment having mass number A and z is the semi-major axis related to the deformation parameter (β) as described below.

According to the pre-scission bending mode oscillation model [2,8] the average angular momentum of the fragment is given as

$$J_{\rm av} = \sqrt{\pi}/2\gamma - 0.5, \qquad J_{\rm av} = (\sqrt{\pi}/2)J_{\rm rms}\,, \tag{4}$$

where γ is the bending oscillation amplitude or the angular positional uncertainty. γ is related to the neck radius (c) and semi-major axis (z) at deformation (β) as [42]

$$\gamma = c/z, \quad z = R(\beta)[1 + (\sqrt{5}/4\pi)\beta], \tag{5}$$

where $R(\beta)$ is the radius considering volume conservation given as

$$R(\beta) = R[1 - (15/16\pi)\beta^2 + 0.25(5/4\pi)^{3/2}\beta^2]^{-1/3}\,. \tag{6}$$

The neck radius c can also be related to the deformation parameter (β) through the scission point distance (D) and thus with the fragment kinetic energy ($E_{\rm K}^{\rm f}$) on the basis of the condition [25] of equality of the Coulomb and nuclear forces at scission point as

$$Z(Z_{\rm F} - Z)e^2/D = 2\pi c^2\Omega/\lambda, \quad D = z_1 + z_2\,, \tag{7}$$

$$E_{\rm K}^{\rm f} = (1 - A/A_{\rm F})E, \quad E = Z(Z_{\rm F} - Z)e^2/D\,, \tag{8}$$

where Ω and λ are the coefficient and range of attractive nuclear force, usually taken as $1.107\,{\rm MeV/F}^2$ and 0.68 F, respectively [43]. $A_{\rm F}$ and $Z_{\rm F}$ are the mass and charge of the fissioning nucleus and E is the total kinetic energy.

It is clear from the above equations (1) and (2) that the calculation of the deformation parameter (β) for a given fragment from the angular momentum ($J_{\rm rms}$) requires the knowledge of temperature (T) for the corresponding split. On the other hand, it can be seen from eqs. (4) and (5) that the calculation of the β-value for a given fragment from its $J_{\rm rms}$-value requires the knowledge of the neck radius c, for the corresponding split. Wilhelmy *et al.* [8] have shown that the c-value is in the range of 1.0 to 1.6 F, whereas Wilkins *et al.* [44] have shown that T might be 1.0 MeV. They have also shown that the fragment deformation (β) (0.95 times Bohr-Mottelson parameter) varies up to 1.0 for various fragments. In view of this consideration, $J_{\rm rms}$ for each fragment was calculated within $1\,\hbar$ of experimental value using statistical correlation and bending oscillation models by varying β from 0.001 to 1.0, T from 0.3 to 2.0 MeV and c from 0.5 to 2.0 F, respectively. Thus, the c and T values resulting in the approximate fragment $J_{\rm rms}$ for each β-value were deduced. Consequently, for each value of c, the kinetic energy (K.E.) for that particular split was calculated using eqs. (7) and (8). The appropriate values of β, T and c for a fragment were then sorted out by comparing the calculated kinetic energy with the experimental value [45]. Since the experimental K.E. data for the individual splits as a function of the charge for a fixed mass is not known, the data corresponding to a fixed mass irrespective of charge was used. Again, since K.E. values of the fast neutron-induced fission of ^{243}Am are not available, the data from thermal neutron-induced fission of ^{243}Am [45] were used with the assumption that the values are the same for thermal and fast neutron-induced fission. In the calculation of the β-values of the odd-Z fragments the contribution of about $2\,\hbar$ from the single-particle spin effect was taken care of. The possible contribution due to post-scission Coulomb torque was not considered as this is evaluated to be with in 1–2 $\hbar$, which

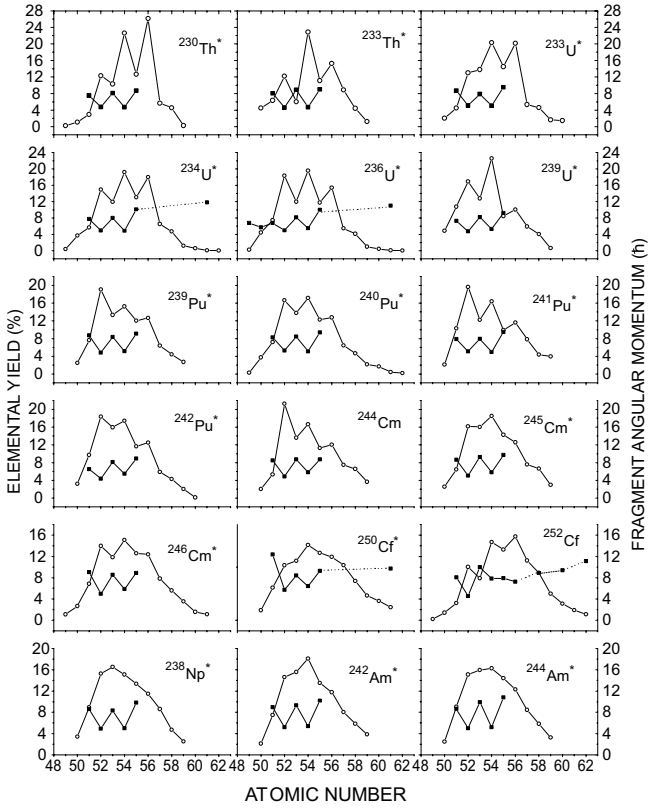

Fig. 3. Plot of the yield-weighed average fragment angular momenta and elemental yields as a function of the atomic number in fifteen even-Z fissioning systems and three odd-Z fissioning systems in the last column. (The open circle corresponds to the elemental yields and the filled square corresponds to the yield-weighted angular momenta of the different elements).

is the same as the uncertainty of the experimental $J_{\rm rms}$-value. Another reason for not considering the contribution from the post-scission Coulomb torque is that it increases with increase of the Coulomb parameter. The deformation parameter (β), neck radius (c), nuclear temperature (T), calculated K.E. data and experimental values are given in table 1.

From table 1 the β-values of the fragments are compared with the corresponding values deduced from the static-scission point model [44] and are found to be in good agreement, which show the validity of the present calculations. It can also be seen from table 1 that the β-values for even-Z fragments corresponding to the products ^{131,133}Te and ^{135}Xe are lower than the adjacent odd-Z fragments corresponding to the products ^{128,130,132}Sb, ^{132,134,136}I and ^{138}Cs. Further comparison of the present and earlier data [30] in the odd-Z fissioning systems (^{238}Np* and ^{242,244}Am*) with the similar data in the even-Z fissioning systems (^{230,233}Th*, ^{233,234,236,239}U*, ^{239,240,241,242}Pu*, ^{244}Cm(SF), ^{245,246}Cm*, ^{250}Cf* and ^{252}Cf(SF)) from the literature [25–29] shows that the β-values of the even-Z fragments are comparable in both even-Z and odd-Z fissioning systems. However, the β-values of odd-Z fragments are slightly higher in the odd-Z fissioning systems than in their adjacent even-Z fissioning systems. This is most probably due to the fact that odd-Z fragments in the odd-Z fissioning systems are more deformed at the cost of their even-Z complementary fragments. Besides this, the single-particle spin from the odd-Z fissioning systems might contribute to the fragment angular momentum and thus increases their deformation. Irrespective of this, the odd-Z fragments always have higher deformation and thus higher angular momentum for both odd-Z and even-Z fissioning systems. Higher deformations of the odd-Z fragments are expected to have higher deformation energy ($E_{\rm D}$) and thus lower intrinsic excitation energy ($E_{\rm i}$). This can be explained from the point of conservation of the Q-value as K.E. and excitation energy (E^*) given as

$$Q = \text{K.E.} + E^* \quad \text{and} \quad E^* = E_{\rm D} + E_{\rm i}\,. \tag{9}$$

For the adjacent split the Q-value, K.E. and E^* are close to each other. Thus, for a fixed value of Q and K.E., higher values of deformation energy ($E_{\rm D}$) for the odd-Z fragment have lower intrinsic excitation energy ($E_{\rm i}$) and vice versa, which reflect in their yields. In order to examine this aspect, the yield-weighted average angular momentum of various fissioning systems from table 2 and their elemental yields from the literature [32,46–49] are plotted in fig. 3. It can be seen from fig. 3 that the angular momentum shows an anti-correlation with the elemental yield in all the even-Z fissioning systems but not in any of the odd-Z fissioning systems, which can be explained as follows.

In the angular-momentum profile the odd-even effect is observed for both even-Z and odd-Z fissioning systems. This is because in both types of fissioning systems odd-Z fragments have a higher fragment angular momentum due to a higher deformation resulting from the core polarization of the even-Z core by the odd proton [41] as mentioned in the text earlier. Besides this, additional spin from the odd proton in the case of odd-Z fissioning systems also contributes to the odd-Z fragments. This results in a higher angular momentum of the odd-Z fragments compared to their adjacent even-Z fragments in both types of fissioning systems. Thus the odd-even effect is found on the angular momentum profile for both even-Z and odd-Z fissioning systems. In the case of the elemental yield profile, the even-odd effect was observed for the even-Z fissioning systems [46–49] but not for the odd-Z fissioning systems [31,32]. This is because in the even-Z fissioning systems either the splits are even-even or odd-odd, whereas in the odd-Z fissioning systems all the splits are even-odd. Based on the static-scission point model [44] in the even-Z fissioning systems the odd-odd split has a higher potential energy at scission, resulting in a lower yield compared to their adjacent even-even splits. This results in the even-odd effect in the elemental yield profile for even-Z fissioning systems [46–49]. In the odd-Z fissioning systems all the splits are even-odd and thus the intrinsic excitation energy for adjacent splits is comparable or very slightly different. This results in negligible or no even-odd effect in the elemental yield profile for odd-Z fissioning systems [31,32]. As a result an anti-correlation

between elemental yields and yield-weighted angular momentum is observed in even-Z fissioning systems but not in odd-Z fissioning systems. This observation indicates the coupling between collective and intrinsic degrees of freedom in both even-Z and odd-Z fissioning systems. Further from fig. 3 it can be seen that the odd-even effect on the yield-weighted fragment angular momentum remains almost constant for both even-Z and odd-Z fissioning systems. However, the even-odd effect on the elemental profile decreases exponentially for the even-Z fissioning systems from Th to Cf [47–49] and it was found to be absent in the odd-Z fissioning systems [31,32]. As a result, a different extent of anti-correlation between elemental yields and yield-weighted fragment angular momentum in even-Z fissioning systems and no anti-correlation in odd-Z fissioning systems were observed. This is because the fragment angular momentum of the fission fragment depends linearly on its deformation and thus with its deformation energy besides single-particle spin contribution from fragment and/or from fissioning systems. Thus, the deformation energy for odd-Z fragments is higher than that of even-Z fragments in any of the fissioning systems. However, the deformation energy of similar types of fission fragments is comparable or slightly different in adjacent even-Z and odd-Z fissioning systems. As a result, a similar or slightly different odd-even effect on the fragment $J_{\rm rms}$ was found in the adjacent even-Z and odd-Z fissioning systems. On the other hand, the yields profile depends exponentially on the intrinsic excitation energy, which is more for even-even splits than for adjacent odd-odd splits in even-Z fissioning systems. Besides this, the average intrinsic excitation energy increases from Th to Cf [47–49]. As a result the even-odd effect on the elemental yield profile in the even-Z fissioning systems decreases exponentially from Th to Cf [47–49]. In the odd-Z fissioning systems the absence or a very feeble even-odd effect on the elemental yield profile is observed due to the availability of comparable or only slight difference in the intrinsic excitation energy for adjacent splits. Thus, a different extent of anti-correlation between elemental yields and yield-weighted fragment angular momentum in even-Z fissioning systems and no anti-correlation in odd-Z fissioning systems are explained. This observation indicates that the extent of coupling between collective and intrinsic degrees of freedom is different in various even-Z fissioning systems. This also indicates that the coupling between collective and intrinsic degrees of freedom is different in even-Z and odd-Z fissioning systems.

Conclusions

i) The fragment angular momentum depends on nuclear-structure effects such as shell closure proximity and odd-even effect. The higher angular momentum of the odd-Z fragment compared to the even-Z fragment is due to the single-particle spin effect or the higher deformation resulting from the strong core polarization of the even-Z core by the odd proton.

ii) For even-Z fragments the $J_{\rm rms}$- and β-values are comparable in both even-Z and odd-Z fissioning systems. However, for odd-Z fragments they are slightly higher in the odd-Z fissioning systems than in their adjacent even-Z fissioning systems. This may be due to the higher deformation of the odd-Z fragments at the cost of their even-Z complementary or may be due to the single-particle proton spin contribution of the odd-Z fissioning systems to the odd-Z fragments.

iii) The fragment deformation at the scission point deduced from the fission fragment angular momentum is seen to be in good agreement with the theoretical value deduced from the static-scission point model.

iv) The yield-weighted fragment angular momentum and the elemental yields profile show an anti-correlation in the even-Z fissioning systems but not in the odd-Z fissioning systems. This is because of the linear dependence of the fragment angular momentum with deformation and thus with deformation energy and of the exponential dependence of the elemental yields with intrinsic excitation energy. This observation indicates that the extent of coupling between collective and intrinsic degrees of freedom in even-Z and odd-Z fissioning systems is different.

The authors thank Dr. V.K. Manchanda, Head, Radiochemistry Division, for his keen interest and encouragement in this work. Thanks are also to due to Dr. R.M. Sawant, Radioanalytical Chemistry Section, for his assistance and to the instrumentation group for their help in maintaining the instruments during the work.

References

1. J.R. Nix, W.J. Swiatecki, Nucl. Phys. **71**, 1 (1965).
2. J.O. Rasmussen, W. Norenberg, H.J. Mang, Nucl. Phys. A **136**, 465 (1969).
3. M.M. Hoffman, Phys. Rev. **133**, B714 (1964).
4. V.M. Strutinski, Sov. Phys. JETP **10**, 613 (1960).
5. H. Nifenecker, C. Signarbieux, M. Ribrag, J. Poitou, J. Matuszek, Nucl. Phys. A **189**, 285 (1972).
6. P. Armbruster, H. Labus, K. Reichelt, Z. Naturforsch. A **269**, 512 (1971).
7. F. Pleasonton, R.L. Ferguson, H.W. Schmitt, Phys. Rev. C **6**, 1023 (1972).
8. J.B. Wilhelmy, E. Cheifetz, R.C. Jared, S.G. Thompson, H.R. Bowman, J.O. Rasmussen, Phys. Rev. C **5**, 2041 (1972).
9. G.M. Ter-Akopian, J.H. Hamilton, Yu. Ts. Oganessian, A.V. Danniel, J. Kormicki, A.V. Ramayya, G.S. Popeko, B.R.S. Babu, Q.-H. Lu, K. Butler-Moore, W.C. Ma, E.F. Jones, J.K. Deng, D. Kliman, J. Shi, M. Morhac, J.D. Cole, R. Aryaeinejad, N.R. Johnson, I.Y. Lee, F.K. Mc-Gowan, Phys. Rev. C **55**, 1146 (1997).
10. M. Jandel, J. Kliman, M. Morhak, J.H. Hamilton, J. Kormicki, A.V. Ramayya, J.K. Hwang, Y.X. Luo, D. Fong, P. Gore, G.M. Ter-Akopian, Yu. Ts. Oganessian, A.M. Rodin, A.S. Fomichev, G.S. Popeko, A.V. Daniel, J.O. Rasmussen, A.O. Macchiavelli, M.A. Stoyer, R. Donangelo, J.D. Cole, Eur. Phys. J. A **24**, 373 (2005).

11. J.P. Bocquet, F. Schussler, E. Monnand, K. Sistemich, *Proceedings of the Fourth IAEA Symposium on Physics and Chemistry of Fission, Julich, Germany*, Vol. **II** (IAEA, Vienna, 1979) p. 179.
12. H.O. Denschlag, H. Braun, W. Faubel, G. Fischbach, H. Meixler, G. Paffrath, W. Porsch, M. Weis, H. Schrader, G. Siegert, J. Blachot, Z.B. Alfassi, H.N. Erten, T. Izak-Biran, T. Tamai, A.C. Wahl, K. Wolfsberg, *Proceedings of the Fourth IAEA Symposium on Physics and Chemistry of Fission, Julich, Germany*, Vol. **II** (IAEA, Vienna, 1979) p. 153.
13. H.O. Denschlag, *Proceedings of the Symposium on Radiochemistry and Radiation Chemistry, IGKAR, Kalpakam, India* (1989) p. IT-10.
14. G. Rudstam, P. Agaard, B. Ekstrom, E. Lund, H. Gokturk, H.U. Zwicky, Radiochim. Acta **49**, 155 (1990).
15. D.G. Sarantites, G.E. Gordon, C.D. Coryel, Phys. Rev. **138**, B353 (1965).
16. D.C. Auman, W. Guckel, E. Nirschl, H. Zeising, Phys. Rev. C **16**, 254 (1977); H. Umezawa, J. Inorg. Nucl. Chem. **35**, 353 (1973).
17. T. Datta, S.P. Dange, A.G.C. Nair, Satya Prakash, M.V. Ramaniah, Phys. Rev. C **25**, 358 (1982).
18. G.P. Ford, K. Wolfsberg, B.R. Erdal, Phys. Rev. C **30**, 195 (1984).
19. N. Imanishi, I. Fujiwara, T. Nishi, Nucl. Phys. A **263**, 141 (1976).
20. I. Fujiwara, N. Imanishi, T. Nishi, J. Phys. Soc. Jpn. **51**, 1713 (1982).
21. B.S. Tomar, A. Goswami, S.K. Das, T. Datta, Satya Prakash, M.V. Ramaniah, Radiochim. Acta **39**, 1 (1985).
22. B.S. Tomar, A. Goswami, A.V.R. Reddy, S.K. Das, S.B. Manohah, Satya Prakash, Radiochim. Acta **55**, 173 (1991).
23. S.P. Dange, H. Naik, T. Datta, R. Guin, Satya Prakash, M.V. Ramaniah, J. Radioanal. Nucl. Chem. Lett. **108**, 269 (1986).
24. S.P. Dange, H. Naik, T. Datta, A.V.R. Reddy, Satya Prakash, M.V. Ramaniah, Radiochim. Acta **39**, 127 (1986).
25. T. Datta, S.P. Dange, S.K. Das, Satya Prakash, M.V. Ramaniah, Z. Phys. A **324**, 81 (1986).
26. H. Naik, R.J. Singh, S.P. Dange, Radiochim. Acta **91**, 1 (2003).
27. H. Naik, T. Datta, S.P. Dange, P.K. Pujari, Satya Prakash, M.V. Ramaniah, Z. Phys. A **331**, 335 (1988).
28. H. Naik, S.P. Dange, R.J. Singh, T. Datta, Nucl. Phys. A **587**, 273 (1995).
29. H. Naik, S.P. Dange, R.J. Singh, Phys. Rev. C **71**, 014304 (2005).
30. H. Naik, S.P. Dange, R.J. Singh, Eur. Phys. J. A **7**, 377 (2000).
31. G. Martinez, G. Barreau, A. Sicre, T.P. Doan, P. Audouard, B. Leroux, W. Arafa, R. Brissot, J.P. Bocquet, R. Faust, F. Koczon, M. Mutterer, F. Gonnenwein, M. Asghar, U. Quade, K. Rudolph, D. Engelhardt, E. piasecki, Nucl. Phys. A **515**, 433 (1990).
32. H. Naik, S.P. Dange, A.V.R. Reddy, Nucl. Phys. A **781**, 1 (2007).
33. K. Flynn, Argonne National Laboratory Report ANL 75-25 (1975).
34. R.H. Iyer, H. Naik, A.K. Pandey, P.C. Kalsi, R.J. Singh, A. Ramaswami, A.G.C. Nair, Nucl. Science Eng. **135**, 227 (2000).
35. E. Browne, R.B. Firestone, *Table of Radioactive Isotopes*, edited by V.S. Shirley (Wiley, New York, 1986).
36. J. Blachot, Ch. Fiche, Ann. Phys. **6**, 3 (1981).
37. J.G. Cunningham, J. Inorg. Nucl. Chem. **4**, 1 (1957); R.R. Pickard, C.F. Goeking, E.I. Wyatt, Nucl. Sci. Eng. **23**, 115 (1965).
38. M.N. Nambodiri, N. Ravindran, M. Rajagopalan Rajkishore, M.V. Ramaniah, J. Inorg. Nucl. Chem. **30**, 2305 (1968).
39. R. Stella, L.G. Moretto, V. Maxia, M. Dicasa, V. Crepsi, M.A. Roller, J. Inorg. Nucl. Chem. **31**, 3739 (1969); M.J. Bennett, W.E. Stein, Phys. Rev. **156**, 1277 (1967).
40. J.R. Huizenga, R. Vandenbosch, Phys. Rev. **120**, 1305, 1313 (1960); W.L. Hafner jr, J.R. Huizenga, R. Vandenbosch, Argonne National Laboratory Report ANL-6662 (1962).
41. V.A. Madsen, V.R. Brown, Phys. Rev. Lett. **52**, 176 (1982); V.A. Madsen, V.R. Brown, J.D. Anderson, Phys. Rev. C **12**, 1205 (1975).
42. H. Schultheis, R. Schultheis, Phys. Rev. C **18**, 1317 (1978).
43. K.T.R. Davies, A.J. Sierk, J.R. Nix, Phys. Rev. C **13**, 2385 (1976).
44. B.D. Wilkins, E.P. Steinberg, R.R. Chasman, Phys. Rev. C **14**, 1832 (1976).
45. M. Asghar, F. Cautucoli, P. Perrin, G. Barreau, B. Leroux, Nucl. Phys. A **334**, 327 (1980).
46. A.C. Wahl, At. Data Nucl. Data Tables **39**, 1 (1988).
47. H. Naik, S.P. Dange, R.J. Singh, S.B. Manohar, Nucl. Phys. A **612**, 143 (1997).
48. H. Naik, R.J. Singh, R.H. Iyer, Eur. Phys. J. A **16**, 495 (2003).
49. H. Naik, R.J. Singh, R.H. Iyer, J. Phys. G. (Nucl. Part. Phys.) **30**, 107 (2004).